Influence of Plate Thickness on the Mechanical Properties of Welded Joints Subjected to Long-Term Postweld Heat Treatments

G. Pimenta and F. Bastian

(Submitted 3 December 2001)

During their service lives, storage spheres, pressure vessels, and other welded structures are subjected frequently to postweld heat treatments (PWHT). Repeated treatments may result, in some cases, in a reduction in mechanical strength and fracture toughness of the weldments such that their mechanical properties may not meet the code specifications after those treatments. Steel ASTM-A-516 Gr 70 is used frequently to build storage spheres and pressure vessels in the petrochemical industry. In this context, the thickness of the plate is an important variable relative to the mechanical behavior of the welded joint after repeated PWHT. In a previous work (Pimenta and Bastian, *JMEPEG,* 2001, *10*, pp. 192-202), the effect of the duration of a PWHT on the mechanical properties of a 65 mm thick plate was evaluated. In the present work, the effect of the same heat treatment on the properties of a 46.4 mm thick plate was evaluated and compared with those of the 65 mm thick plate. For this purpose, hardness measurements, tensile and Charpy V-notch impact tests, and a metallographic analysis were performed. The results show that both the base metal and heat-affected zone of the thinner plate present higher mechanical strength and impact resistance for all heat-treated conditions. The obtained mechanical properties were then compared with the requirements of the ASME Code, Section VIII.

Keywords mechanical properties, plate thickness, postweld heat treatments, pressure vessel steel

1. Introduction

During their service lives, storage spheres, pressure vessels, and other welded structures are subjected frequently to postweld heat treatments. Repeated treatments may result, in some cases, in a reduction in mechanical strength and fracture toughness of the weldments such that their mechanical properties may not meet the code specifications after those treatments. For instance, pressure vessels and spheres used for the storage of liquid petroleum gas, propane, and butane are susceptible to the formation of cracks in the welded joints during their service life. These cracks in the welds and heat-affected zones (HAZs) of the joints can run as large as 25 mm long and 3 mm deep to 1000 mm long and 12 mm deep.[1]

There are several types of spheres worldwide with a relatively high number of cracks. Most of these spheres were fabricated using steels of the specification ASTM A-516 Gr. 70[2] and fabricated following the ASME Code, Section VIII, Divisions 1 and 2.[3] Some of these spheres were already subjected to more than two heat treatments, which followed the repair of the defects, sometimes above that which is allowed by the standard.

There are several disparities among the international standards for specification of the thermal cycle in stress-relief heat treatments for carbon-manganese and microalloyed steels: all are lacking in relation to the number of thermal cycles a structure can withstand while maintaining an acceptable level of mechanical properties.

In a previous work,[4] the effect of the time of the stress-relief heat treatment at 620 °C on the tensile properties, hardness, and impact resistance of a welded joint of a 65 mm thick plate (ASTM A-516 Gr. 70) was studied. In the present work, the effect of the same heat treatments on properties of a welded joint of a 46.4 mm thick plate of the same steel was evaluated. A comparison of the properties of this plate and those of the plate of 65 mm also was performed.

2. Materials

2.1 Steels Studied

A steel plate (ASTM A-516 Gr 70) with a thickness of 46.4 mm was used in the work. Table 1 presents the chemical composition of this steel, as well as that of the 65 mm thick plate used in the previous work [1]. A comparison of the properties of both plates also was performed. The 46.4 mm thick plate is designated Plate 1 (P1), whereas the 65 mm thick plate is Plate 2 (P2).

Table 1 Chemical Composition of the Steels Studied

	Chemical Composition (wt.%)							
Element	**C**	**Si**	**Mn**	**Al**	**Ni**	**Ti**	**S**	**P**
Plate 1 (P1)	0.24	0.25	0.99	0.02	0.04	0.01	0.006	0.020
Plate 2 (P2)	0.25	0.24	1.00	0.05	0.07	0.01	0.015	0.018

G. Pimenta, Petrobras-Cenpes, Quadra 7, Ilha do Fundão, 21949-900, Rio de Janeiro, RJ, Brazil; and **F. Bastian,** COPPE/UFRJ, Metallurgical and Materials Engineering, Caixa Postal 68505, Rio de Janeiro, 21945-970, Brazil. Contact e-mail: fbastian@metalmat.ufrj.edu.br.

Table 2 Welding Parameters

Electrode	E-7018 (iron powder, low hydrogen)
Joint geometry	Type K
Polarity	Inverse
Type of current	Continuous
Welding speed	10 to 18 cm/min
Welding position	Flat position
Interpass temperature	250 °C (maximum)
Preheating temperature	125 °C (minimum)
Electrode diameter	
Root	3.25 mm
Filler	4.00 mm
Welding current	
Root	75–120 A
Filler	
Arc voltage	120–125 A
Root	20–25 V
Filler	22–27 V

2.2 Welding Procedure

For the study, welded K-type joints were used to produce a uniform HAZ parallel to the flat side of the joint. The welding procedure followed the standard ASME/AWS.[5] The welding parameters are presented in Table 2.

Strips 300 mm wide were cut parallel to the rolling direction of the plates and welded in pairs along the cut edges. The shielded metal arc welding operation was performed by welders qualified following the ASME standard. The welded joints were inspected using penetrant liquid in the root pass, in both sides of the joint, and visual inspection of the filling passes after cleaning. After the welding operation, the welded joints were inspected by gammagraphy. Some regions were also inspected by ultrasound.

2.3 Stress-Relief Heat Treatments

Strips of the base metal (BM) and welded strips were treated in an electric resistance industrial furnace with programmable control of temperature. The temperature of the treatment was 620 ± 5 °C. The specimens were maintained at this temperature range for continuous time periods of 2.3, 6.3, 14.2, and 21.2 h for 1, 3, 6, and 10 heat treatments, respectively. The heating rate was 220 °C/h in maximum (above 315 °C) and the cooling rate was 260 °C/h in maximum (until 315 °C, and then cooling in air).

3. Experimental Methods

3.1 Macrographic Examination

Two samples, 10 mm wide and 100 mm long, were cut from each heat-treated plate for macrographic examination and measurement of hardness. After polishing, the samples were etched with a Nital 2 etchant (ethilic alcohol with 2% in volume of nitric acid) to check for the uniformity of the weld groove and the HAZ.

3.2 Metallography

A metallographic analysis was performed to characterize the microstructures resulting from the different heat treatments.

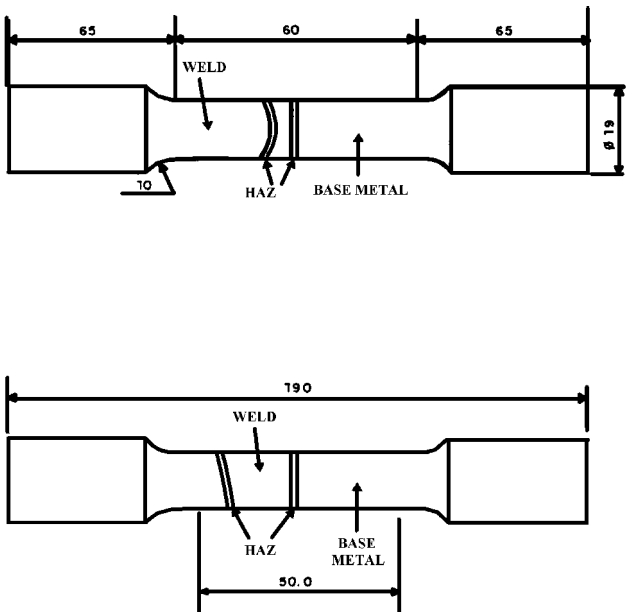

Fig. 1 Tensile testpiece of the welded joint. The testpiece was taken from the half-thickness region of the plate. Dimensions are in millimeters.

A Nital solution was used to etch the samples. An optical microscope model DI–12-32 75057 (Carl Zeiss, Germany) and a scanning electron microscope JEOL model JXA 8440A (Japan Electron Optics Ltd., Tokyo) were used for the observations.

3.3 Tensile Testing

The tensile tests were performed following the standard ASTM E 8M[6] in a screw-driven Panambra model 100 TU2634 (Panambra Industrial e Técnica SA, São Paulo) universal testing machine of 200 MN with an electronic extensometer. The tensile testpieces had a circular section with the dimensions shown in Fig. 1. They were cut transversally to the rolling direction at half-thickness. Specimens from the BM and the welded joints were tested at room temperature. At least three specimens were tested for each heat-treatment condition.

3.4 Hardness Measurements

The Rockwell A hardness (RAHN)[7] of the samples was measured at a distance of 5 mm from the surface of the plates, at half-thickness and along the HAZ. The macrographic samples were used for this purpose. The Vickers microhardness (VHN)[8] was also evaluated in the same regions of the measurements of RAHN.

3.5 Charpy-V-Notch Impact Testing

The Charpy impact tests were performed following the standard E-23.[9] The notches were machined in the fusion line of the HAZ and in the BM, parallel to the rolling direction, as shown in Fig. 2, corresponding to the orientation T-L of the standard ASTM E 616.[10] The tests were performed at tem-

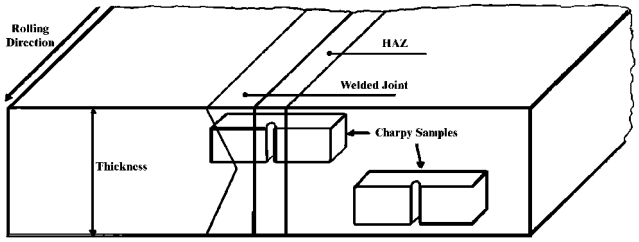

Fig. 2 Location of the Charpy testpieces

peratures of 40, 23, 0, −10, −20, −40, and −60 °C. A mixture of liquid nitrogen and ethilic alcohol was used. Four testpieces were used for each temperature. The samples taken from the welded joints were etched in a solution of Nital 2 to reveal the HAZ, allowing location of the machined notch. A Tokyo impact testing machine, model EC-30, was used.

3.6 Fractography

A fractographic analysis of the Charpy testpieces with absorbed impact energy at fracture below 30 J was performed using the JEOL scanning electron microscope mentioned previously.

4. Experimental Results

4.1 Macrography

Prior to making the mechanical tests, a macrographic examination of sections taken from the welded joints was performed to check for the uniformity of the welds and HAZs. A macrographic examination was also performed to check whether the notches of the Charpy testpieces were correctly located in the HAZs. Figure 3 illustrates the different regions of the welded joint of the work.

4.2 Metallography

Figure 4 shows the microstructure of the BM of P1 and Fig. 5, the microstructure of the BM of P2. They were obtained using the optical microscope at the same magnification. Both were subjected to 2.3 h of treatment. The microstructure of both steels is practically equal to that of the as received condition, being a ferrite-pearlite aggregate with P2 showing a much coarser structure.

The heat treatment at 620 °C for long periods of time promoted a spheroidization and coalescence of the cementite lamella of the pearlite, as shown by the comparison of Fig. 6, which corresponds to the treatment of 2.3 h, and Fig. 7, which corresponds to the treatment of 21.2 h.

A coalescence of the carbide particles of the HAZ also took place as a result of the increase of the holding time at 620 °C, illustrated by Fig. 8 and 9, which correspond to 2.3 and 21.2 h of treatment, respectively.

4.3 Tensile Tests

The results of the tensile tests of the heat-treated 46.4 mm thick plate are shown in Table 3, which also shows the results

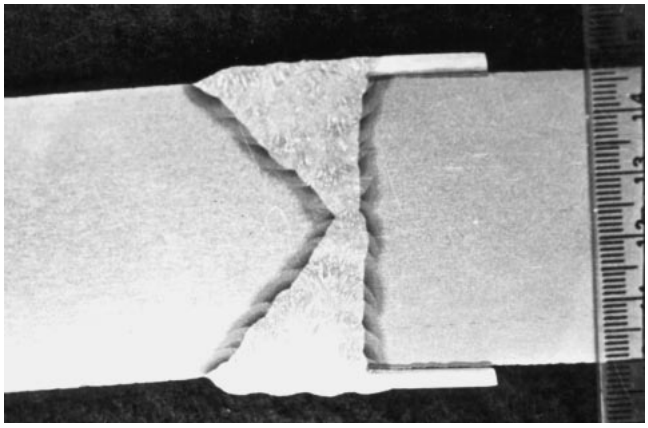

Fig. 3 Macrography of the welded joint. Etching with Nital 2

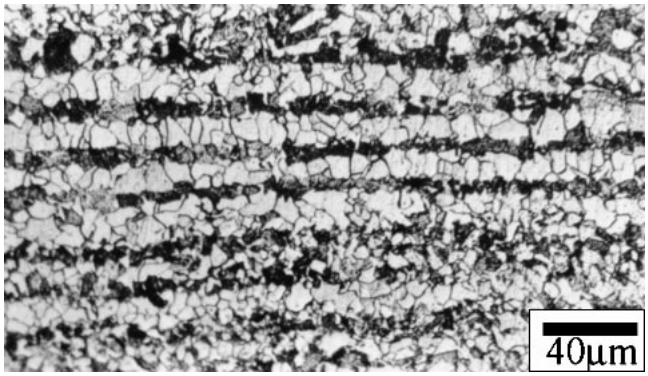

Fig. 4 Microstructure of the BM of P1 heat treated for 2.3 h. Optical microscopy. Nital 2 etching

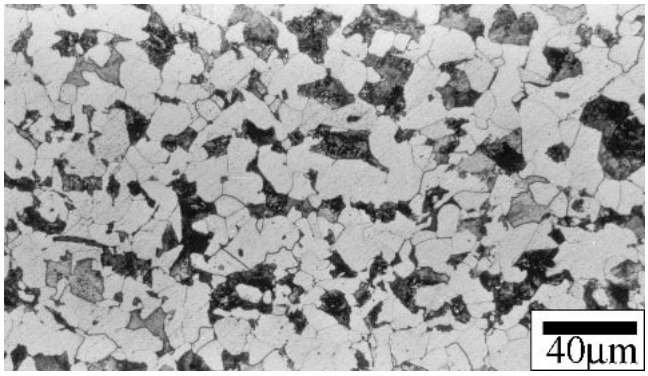

Fig. 5 Microstructure of the BM of P2 heat treated for 2.3 h. Optical microscopy. Nital 2 etching

of the 65 mm thick plate[4] for comparison. It may be noticed that the yield limit (YL) and ultimate tensile stress (UTS) of the BM and HAZ of both plates decreased slightly with the time of heat treatment. A slight increase of elongation and area reduction was observed.

4.4 Hardness Measurements

Hardness measurements were made on the BM and HAZ. The measurements were made 5 mm from the plate surface and

at half-thickness of the plate and along the HAZ, in the flat side of the K joint. Table 4 shows RAHN and VHN for each time of heat treatment for both plates. It shows that there was a small decrease of hardness with the holding time at 620 °C.

4.5 Charpy-V-Notch Impact Testing

The results of the Charpy impact tests of the BM and HAZ of the heat-treated 46.4 mm thick plate are shown in Fig. 10 and 11, respectively. The mean absorbed energies are plotted as a function of the testing temperatures for the different heat treatments. The figures show, for all heat treatments, that the HAZ always presented higher impact energy and lower transition temperature than BM. The impact energy decreased for heat treatments longer than 6.3 h, with the BM presenting a more pronounced decrease. Similar trends were observed for the 65 mm thick plate.

Figures 12 and 13 show the values of mean absorbed impact energy of the BM and HAZ, respectively, as a function of the time of heat treatment for the different testing temperatures. A reference line corresponding to an absorbed energy of 30J is also drawn in the figures.

A comparison of the absorbed energies of the 46.4 and 65 mm thick plates for the same heat treatments and testing tem-

Fig. 6 Microstructure (SEM) of the BM of P1 heat treated for 2.3 h

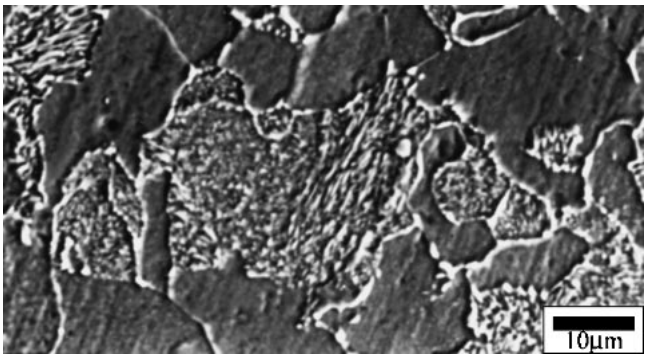

Fig. 7 Microstructure (SEM) of the BM of P1 heat treated for 21.2 h

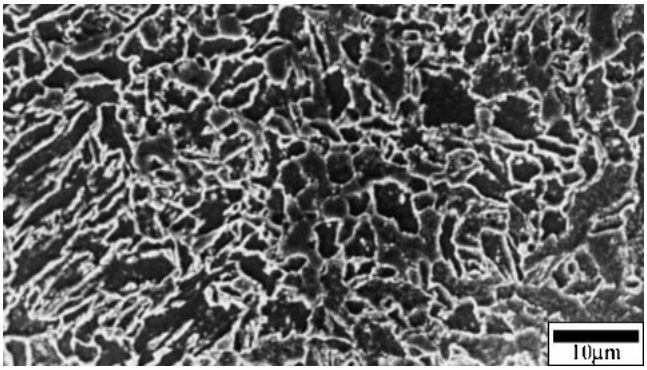

Fig. 8 Microstructure (SEM) of the HAZ of P1 heat treated for 2.3 h

Table 3 Tensile Properties of the BM and Welded Joint of Plate 1 and Plate 2 as a Function of the Time of Treatment at 620 °C

	Time of Heat Treatment (h)			
Tensile Properties	**2.3**	**6.3**	**14.0**	**21.2**
Ultimate tensile stress (MPa)				
Plate 1				
BM	537	534	520	517
HAZ	540	539	527	520
Plate 2				
BM	503	506	487	482
HAZ	516	514	497	474
Yield limit (MPa)				
Plate 1				
BM	341	360	313	298
HAZ	350	350	335	328
Plate 2				
BM	316	306	295	287
HAZ	299	284	275	271
Area reduction (%)				
Plate 1				
BM	36.15	35.20	35.80	36.07
HAZ	35.00	34.10	33.00	31.00
Plate 2				
BM	30.80	34.13	34.60	34.53
HAZ	24.20	25.00	26.80	29.00
Elongation (%)				
Plate 1				
BM	67.13	67.56	67.35	67.90
HAZ	65.00	65.50	66.00	66.20
Plate 2				
BM	54.07	62.00	62.90	64.16
HAZ	57.70	60.80	61.20	61.50

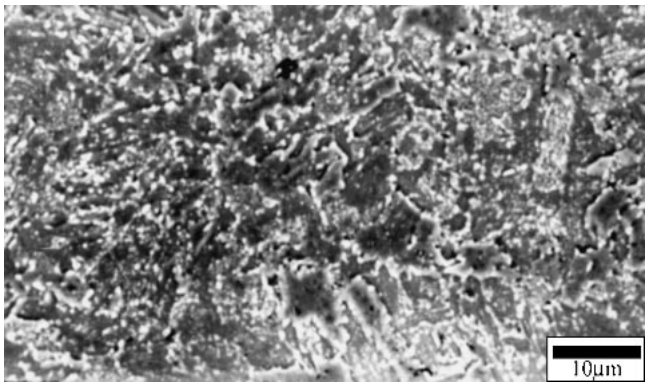

Fig. 9 Microstructure (SEM) of the HAZ of P1 heat treated for 21.2 h

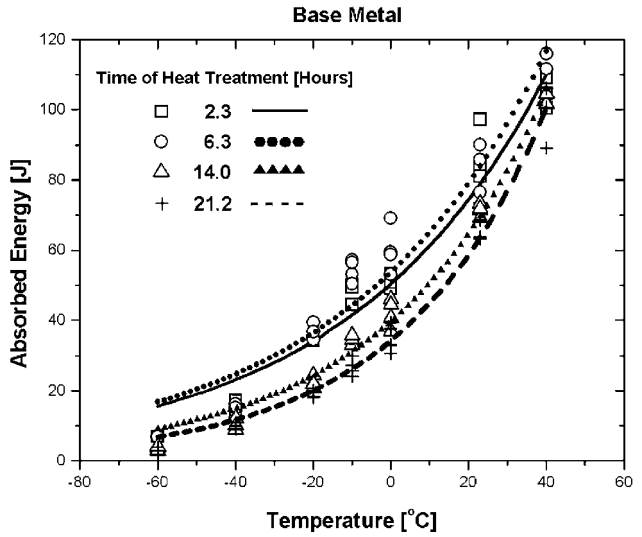

Fig. 10 Charpy absorbed impact energy of the BM for the different heat treatments as a function of the testing temperatures

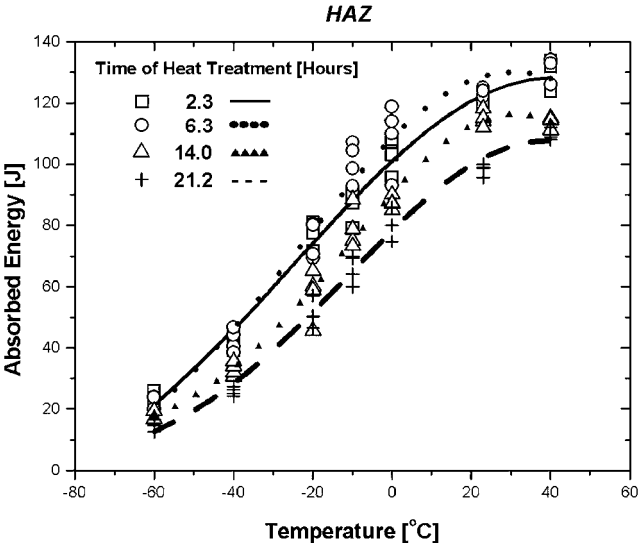

Fig. 11 Charpy absorbed impact energy of the HAZ for the different heat treatments as a function of the testing temperatures

peratures was also performed. Figures 14 to 19 show the results of this comparison. Figures 14 to 16 correspond to the base metal and Fig. 17 to 19 to the HAZ. From Fig. 14 to 16, it is possible to see that for any testing temperature the absorbed energy of the thinner plate P1 is higher than that of P2 for any similar time of heat treatment. This also happens with the welded joint, as shown by Fig. 17 to 19.

Figures 14 to 19 corroborate the fact that the impact resistance of the BM is lower than that of the welded joint, this becoming critical in the case of BM for testing temperatures below 0 °C, especially in the case of P2. The situation of the welded joint is much more comfortable. In this case, both P1 and P2 had values above the 30 J for testing temperatures as low as −20 °C.

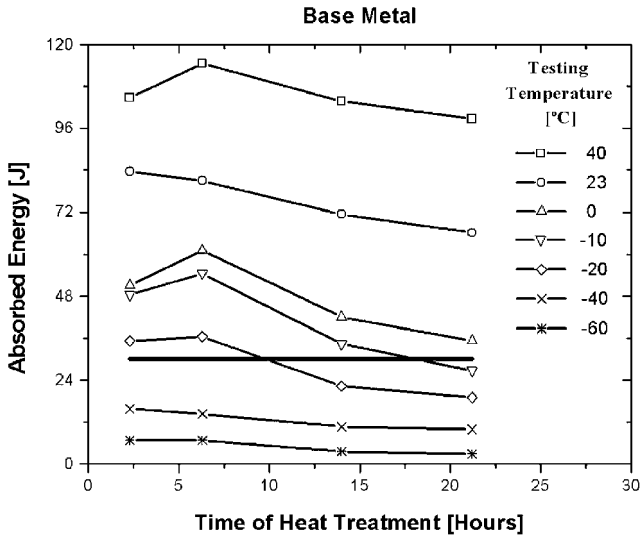

Fig. 12 Charpy absorbed impact energies of the BM of P1 as a function of the time of treatment at 620 °C

5. Discussion

5.1 Tensile Properties

The obtained results show that YL, UTS, and hardness of P1 decreased slightly with the time of heat treatment, similarly to what had also occurred with P2,[4] which was of greater thickness. On the other hand, EL and AR increased slightly with the time of heat treatment. Sparkes,[11] working with C-Mn-Nb and C-Mn-Nb-V pressure vessel steels, observed that their mechanical strength decreased when heat treated above 600 °C. Similar results were obtained by Brito et al., [12] working with an ASTM A 537 C1 steel, which showed a small drop of strength for a heat treatment at 650 °C. A decrease of mechanical strength of the BM of several steels as a result of the prolonged heat treatment was also observed by Konkol.[13]

The standard ASTM-A-516 Gr. 70 specifies the following values for the tensile properties: YL, a minimum of 280 MPa; UTS, 485 to 620 MPa; and EL, a minimum of 21%. The comparison of the required and obtained values for P1 indicates that all the required values were met easily. This was not the case of the thicker plate, P2, the UTS values of which for both BM and HAZ fell below the requirements for the 21.2 h treatment. The same happened with the YL from the HAZ of plate P2, where the requirements were not met.

5.2 Impact Testing

The results obtained from the impact tests with P1 and their comparison with those obtained from P2 allow the following observations:

- For any testing temperature, the impact resistance decreased with the increase of the time of treatment for treatments longer than 6.3 h;
- The ductile-brittle transition temperature increased with the time of heat treatment;

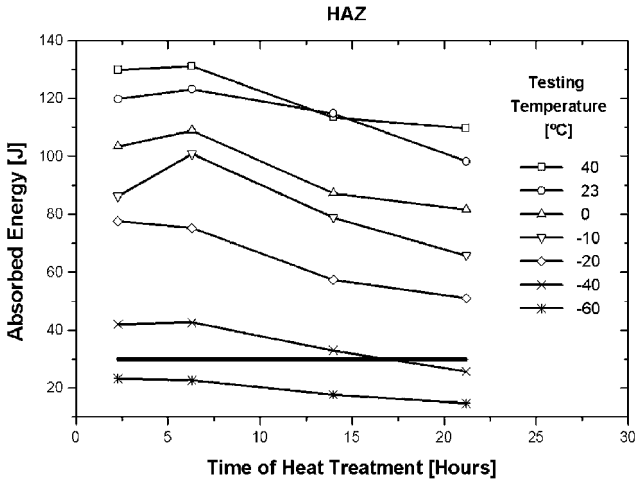

Fig. 13 Charpy absorbed impact energies of the HAZ of P1 as a function of the time of treatment at 620 °C

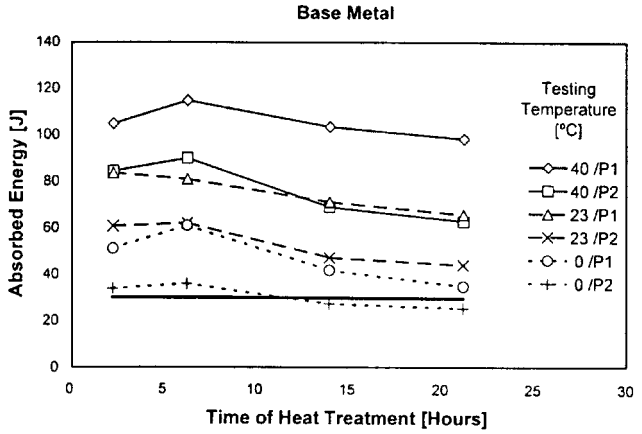

Fig. 14 Charpy absorbed impact energies of the BM of P1 and P2 as a function of the time of heat treatment. Testing temperatures of 40, 23, and 0 °C

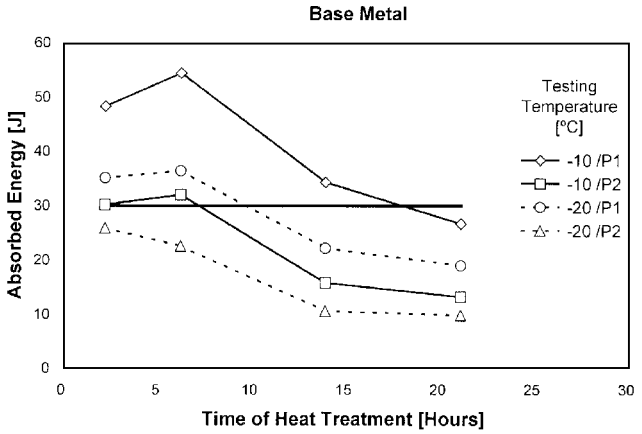

Fig. 15 Charpy absorbed impact energies of the BM of P1 and P2 as a function of the time of heat treatment. Testing temperatures of −10 and −20 °C

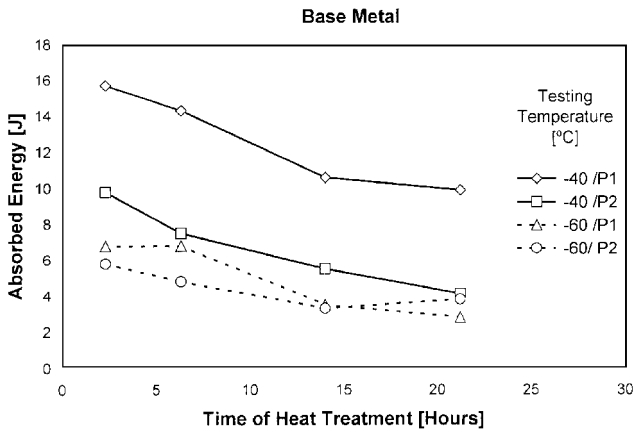

Fig. 16 Charpy absorbed impact energies of the BM of P1 and P2 as a function of the time of heat treatment. Testing temperatures of −40 and −60 °C

Table 4 Hardness Values for the Different Heat Treatments at 620 °C

	Time of Heat Treatment (h)							
	2.3		6.3		14.0		21.2	
Plate	RAHN	VHN	RAHN	VHN	RAHN	VHN	RAHN	VHN
1								
Region								
Surface	50.5	161	50	158	49	150	48	148
Half-thickness	48.5	157	48.5	154	48	147	46	144
HAZ	55	180	54	178	51	167	49	160
2								
Region								
Surface	46	153	45.5	150	45	140	44	139
Half-thickness	45	149	45	148	44	140	42.5	137
HAZ	51	165	51	164	48.5	157	48	150

- The impact resistance of the HAZ was larger than that of the BM;
- For any testing temperature, P1 always presented higher impact resistance than P2.

The results obtained with P1 show the same trends as those obtained with P2, which were discussed previously.[1]

In discussing the influence of plate thickness on its impact resistance, the effect of grain size and impurity level on the

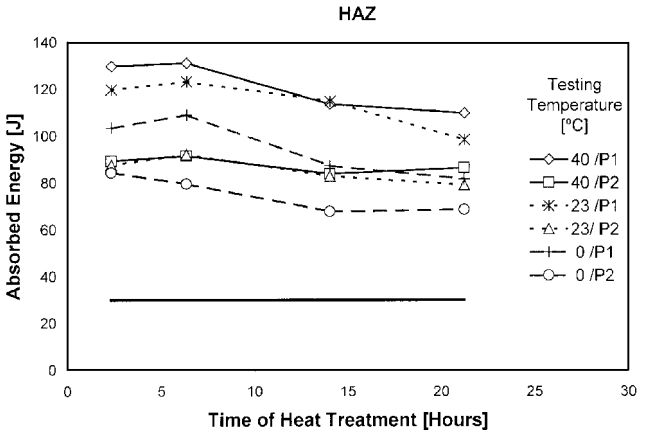

Fig. 17 Charpy absorbed impact energies of the HAZ of P1 and P2 as a function of the time of heat treatment. Testing temperatures of 40, 23, and 0 °C

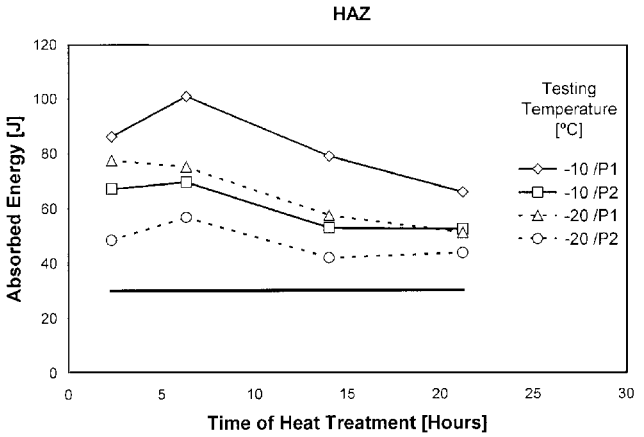

Fig. 18 Charpy absorbed impact energies of the HAZ of P1 and P2 as a function of the time of heat treatment. Testing temperatures of −10 and −20 °C

fracture behavior of welded joints of steel was studied by Doubby[14] and Fairchild and Koo.[15] They observed higher fracture toughness and lower transition temperatures in steels with finer microstructure and small impurity contents. It is well documented in the literature, on the other hand, that thicker plates normally present a coarser microstructure and a tendency to larger impurity content in the central region than thinner plates of the same composition.[16] This is the case of the steels in the present study. Based on this evidence, it is not difficult to explain the worse performance shown by P2.

The ASME Code, Section VIII, Div. 1 requires, for the present material and welding conditions, an energy of 30 J as the minimum average result of three Charpy tests. The minimum individual result specified is 20 J. Figures 14 to 19 show the absorbed energies of P1 and P2 as a function of time of heat treatment for each testing temperature. A line corresponding to a fracture energy of 30 J was also drawn Fig. 14.

From these figures it is possible to observe the following:

- The test temperature for the absorbed energy of 30 J increased with the time of heat treatment, this being more pronounced in the BM of P2;
- Among the test temperatures used in the work, −20 °C was the lowest temperature that allowed all the heat-treated HAZ to be in accordance with the ASME code. In the case of the BM, this temperature was approximately 0 °C.

Konkol[13] studied the influence of changes in the microstructure on the transition temperature of welded joints due to heat treatments. He observed that there was a progressive spheroidization of the carbides with the time of heat treatment for the steels of his study. Other researchers[12,17,18] obtained similar results.

The decrease of fracture toughness due to the spheroidization and coarsening of the cementite of pearlite was also observed by Fairchild et al.[15] when studying the influence of temperature on the stress-relief heat treatment. They observed, using instrumented Charpy tests, an increase in the transition temperature with the temperature of treatment due to pearlite spalling. Figures 6 and 7 of the present work show that there

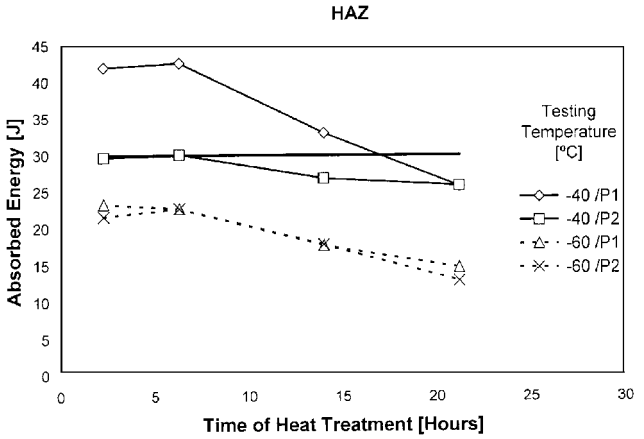

Fig. 19 Charpy absorbed impact energies of the HAZ of P1 and P2 as a function of the time of heat treatment. Testing temperatures of −40 and −60 °C

was a substantial spheroidization of the carbides with the treatment of 21.2 h when compared to the treatment of 2.3 h.

Also important is the observation that the carbides in the BM are not fully spheroidized, presenting regions still with a pearlitic morphology. This is related to the impact behavior of the BM, which presents an increase of transition temperature with the time of treatment.

Multipass welding with adequate parameters, temperature control of preheating and interpasses, and postweld heat treatments are the basic conditions to obtain adequate fracture toughness in the HAZ. When these conditions are met, the final microstructure contains a large fraction of fine-grained acicular ferrite.

The observation of the HAZ of P1 and P2 showed that it is formed of acicular ferrite and plates of aligned carbides with P1 presenting a larger fraction of fine grain regions. The heat treatments promoted a coalescence of the carbides in both plates.

The observation of Fig. 14-16 shows that the impact resistance of the BM of both P1 and P2 decreased in an almost

Fig. 20 Cleavage fracture morphology of a Charpy testpiece of the HAZ of P1 with an absorbed fracture energy below 30 J

similar fashion, indicating that the microstructural changes taking place in the plates are analogous. The same happened with the HAZ, as shown by Fig. 17-19.

The morphology of the fracture surface of the Charpy testpieces at the temperatures in which the absorbed energy was below 30 J was cleavage (Fig. 20).

6. Conclusions

The influence of plate thickness on the mechanical properties of welded joints of an ASTM A-516 Gr. 70 pressure vessel steel subjected to postweld heat treatment at 620 °C for different periods of time was evaluated. The results obtained from hardness measurements, tensile and Charpy V-notch impact tests, and microstructural analysis led to the following conclusions.

The effect of heat treatments for long periods of time was deleterious for both plates: There was a small decrease in hardness and in mechanical strength of the steel, and the ductile-brittle transition temperature increased with the time of heat treatment. The impact resistance decreased for heat treatments longer than 6.3 h. The deterioration of the mechanical properties was due to microstructural changes taking place in the material, mainly spheroidization of the cementite of pearlite and pearlite spalling in the BM and coarsening of the carbides in the HAZ.

Although they followed similar trends, the plates exhibited different performances. The tensile properties of the thinner plate were superior to those of the thicker plate for both the BM and HAZ. Analogously, the impact resistance of P1 was higher at any given testing temperature. The main cause for these differences is attributed to the coarser microstructures and higher impurity content of P2. The comparison of the required and obtained values of the tensile properties of the steel indicates that all the required values were met by P1, irrespective of the heat treatment condition. This is not the case of P2, whose values of mechanical strength fell below the requirements for the 21.2 h treatment.

It is also important that for the welding procedure and postweld heat treatments, the impact resistance of the HAZ was superior to that of the BM for both plates. Among the test temperatures used in the work, −20 °C was the lowest temperature that allowed all the heat-treated HAZ testpieces to be in accordance with the ASME Code, Section VIII. In the case of the BM this temperature was approximately 0 °C.

Acknowledgments

The financial support from CNPq is gratefully acknowledged. The authors thank J.C.G. Teixeira for his helpful comments.

References

1. J.E. Cantwell: *Corrosion 88*, St. Louis, MO, 1988, paper no. 157.
2. *Standard Specification for Pressure Vessel Plates, Carbon Steel for Moderate and Lower Temperature Service*, ASTM A-516, ASTM, Philadelphia, PA, 1993.
3. ASME Boiler and Pressure Vessel Code, Section VIII, Divisions 1 and 2, ASME, Fairfield, NJ, 2001.
4. G. Pimenta and F. Bastian: "Effect of Long-Time Postweld Heat Treatments on the Mechanical Properties of a Carbon-Manganese Pressure Vessel Steel," *JMEPEG,* 2001, *10,* pp. 192-202.
5. *AWS D.1.1-81,* 5th ed., American National Standards Institute, New York, 1981.
6. *Standard Tests Methods for Tension Testing of Metallic Materials [Metric]*, ASTM E 8M, ASTM, Philadelphia, PA, 1989.
7. *Standard Methods for Rockwell Hardness and Rockwell Superficial Hardness of Metallic Materials*, ASTM E 18, ASTM, Philadelphia, PA, 1989.
8. *Standard Methods for Microhardness of Materials,* ASTM E-384*,* ASTM, Philadelphia, PA, 1984.
9. *Standard Methods for Notched Bar Impact Testing of Metallic Materials*, ASTM E 23, ASTM, Philadelphia, PA, 1980.
10. *Standard Terminology Relating to Fracture Testing,* ASTM E 616, Philadelphia, PA, 1982.
11. D.J. Sparkes: *Effect of a Postweld Heat Treatment on HAZ Microstructure and Toughness of Microalloyed C-Mn Submerged–Arc Welds,* TWI Research Report No. 323, TWI, Cambridge, 1986.
12. V.L.O Brito, H.J.C. Voorwald, N. Neves, and I.S. Bott: "Effects of a Postweld Heat Treatment on a Submerged-Arc Welded ASTM A 537 Pressure Vessel Steel," *JMEPEG,* 2001, *10,* pp. 249-57.
13. P.J. Konkol: *Effect of Long-Time Post Weld Heat Treatment on the Properties of Constructional Steel Weldments*, Welding Research Council, No. 330.
14. R.E. Doubby: *HAZ Toughness of Structural and Pressure Vessel Steels—Improvement and Prediction,* Welding Research Council, New York, Aug 1979, pp. 225-37.
15. D.P. Fairchild and J.Y. Koo: "The Effects of Post Weld Heat Treatment on the Microstructure and Toughness of Offshore Platform Steels," in *Proc. of the 6th International Offshore Mechanics and Arctic Engineering Symposium,* vol. III, M.M. Salama, H.C. Rhee, and J.K. Koo, ed., ASME, Houston, TX, 1987, pp. 121-29.
16. M*etals Handbook*, 9th ed., vol. 1., ASM Metals Park, OH, 1978.
17. R.D. Stout: *Postweld Heat Treatment of Pressure Vessels,* Welding Research Council, New York, 1985, No. 305.
18. P.L. Threadgill and R.H. Leggatt: *Effects of Postweld Heat Treatment on Mechanical Properties and Residual Stress Levels of Submerged–Arc Welds in a C-Mn-Nb-Al Steel*, TWI Research Report No. 253, TWI, Cambridge, 1984.